

Diamond Surface Conductivity under Atmospheric Conditions: Theoretical Approach

Karin Larsson^{*,†} and Juergen Ristein[‡]

Department of Materials Chemistry, Angstrom Laboratory, Box 538, 751 21 Uppsala, Sweden, and
Institute of Technical Physics, University of Erlangen, Erwin-Rommel Strasse 1, 91058 Erlangen, Germany

Received: January 24, 2005; In Final Form: March 16, 2005

The electron transfer from an H-terminated diamond (100)- 2×1 surface to a neutral or acidic water adlayer has been theoretically investigated, using quantum mechanical DFT calculations under periodic boundary conditions. A surface conductivity of p-type was found to be induced by the acidic environment. An electron transfer of 1.8 electrons per surface unit cell was observed to take place from the upper part of the diamond valence band to the lowest unoccupied molecular level of the aqueous adlayer that contains one H_3O^+ ion. The result is a hole delocalized over the whole diamond model slab. Also, a pronounced weakening of the H_3O^+ bonds by the interaction with the diamond surface is observed.

Introduction

A unique feature of undoped thin film of diamond, grown by chemical vapor deposition (CVD), is that it has been found to display p-type surface conductivity. More than 10 years ago, Ravi and Landstrass observed this conductivity on hydrogen-terminated (H-terminated) diamond surfaces.¹ Hayashi et al. later identified the charge carrier type as holes by their hole effect.² This phenomenon has recently attracted a lot of interest since a number of electronic applications proposed for diamond are based on this effect. Various models describing the near-surface layers that give rise to the p-type conductivity have been presented earlier and discussed.^{3–8} Kawarada formally claimed that hypothetical acceptor-like surface states are responsible for the holes, whereas Hayashi proposed that very shallow so-called hydrogen-induced subsurface acceptor states inside the diamond are responsible. They based their proposal on hydrogen profiles obtained on hydrogenated polycrystalline diamond films by secondary-ion mass spectrometry, which showed tailing from the surface into the bulk with 20 nm half-width.⁴ Later, experiments on better defined single-crystal samples by elastic recoil detection analysis (ERDA) with much superior depth resolution came to contradicting conclusions about the existence of subsurface hydrogen.^{9,10} Moreover, despite several theoretical attempts, no microscopic configuration for a hydrogen-related shallow surface or subsurface defect could be found that could serve as a surface acceptor.¹¹ The question of the location of the acceptors responsible for surface conductivity, i.e., whether on top of or below the surface, was recently also investigated by Takeuchi et al. and Ristein et al. via the surface band bending profile that accompanies the charge separation between holes and acceptors.^{12,13} Their results could be easily explained assuming acceptors on the surface, whereas an unrealistic high surface defect density and very sharp subsurface acceptor profiles had to be assumed for any subsurface acceptor model. Maier et al. have proposed another mechanism that involves hydrogen-terminated diamond surfaces in an atmospheric environment.⁶ Their work was based on the observation that chemisorbed hydrogen on the surface is a necessary but not a

sufficient prerequisite for surface conductivity. Instead, additional surface adsorbates are needed that are appropriately provided by a weakly acidic water layer physisorbed on the H-terminated diamond surface. The influence of differing chemical environments on the surface conductive properties of CVD diamond films had first been reported by Ri et al., who found an enhancement of surface conductivity by an acidic ambient and suppression by an alkaline one.¹⁴ These early results were later confirmed by Foord et al.⁷ and also by Vittone et al.¹⁵

The surface conductivity in as-grown chemical vapor deposited diamond films has been shown by Cannaeerts et al. to change significantly after annealing under high vacuum conditions at various temperatures.¹⁶ Such changes were found by several other groups and, as an important result, they were found to be reversible upon reexposure of the samples to air.^{17–19} This observation, that the exposure of H-terminated diamond surfaces to air is a requirement for p-type surface conductivity to occur, has been thoroughly investigated also in the work by Maier et al.⁶ and Mantel et al.²⁰ Surface termination by hydrogen, in addition to at least one physisorbed species, was shown to be responsible for the surface conductivity of diamond (100). Red/ox reactions in a physisorbed water layer were then suggested to provide the electron sink for the holes in the subsurface accumulation layer in diamond. Ristein et al. proposed that electron transfer from the upper part of the valence band to these physisorbed adsorbates was the effective p-type doping mechanism for H-terminated diamond surfaces.²¹ This charge exchange can be regarded as an electrochemical process since the adsorbates are dissolved in a mildly acidic aqueous layer of atmospheric origin on the diamond surface.

The mechanism of surface conductivity has also theoretically been investigated, using density functional theory (DFT) and a cluster approach. The role of dangling bonds and covalently bonded H adsorbates on diamond cluster surfaces was studied by Dai et al. in examining the electronic structures of various cluster sizes.²² The results showed two possible mechanisms for a surface conductivity along the grain boundaries of polycrystalline material. One originates from the transport of electrons in localized states near the Fermi level. The other mechanism originates from the holes in extended states at about the mobility edge. In addition, Goss et al. calculated the electronic properties of isolated molecular adsorbates phys-

* Corresponding author. E-mail: karin.larsson@mkem.uu.se.

[†] Angstrom Laboratory.

[‡] University of Erlangen.

TABLE 1: Evaluation of Hartree–Fock (HF) and Various DFT Functionals with Respect to Hydrogen Bond Strengths (kJ/mol) in Different H₂O Systems: Molecular H₂O–H₂O Interactions and Intermolecular Interactions in Ice (Phase Ih)

	HF	MP2	BLYP	B3LYP	PW91	expt
H ₂ O–H ₂ O	14.8 ^a	15.8 ^a	16.1 ^a	18.3 ^a	21.6 ^a	20.9 ^a
	MP2	RPBE	PBE	PW91	expt	
H ₂ O(s)	24.8 ^b	11.7 ^b	14.9 ^b	17.6 ^b	21 ^c	

^a Tsuzuki, S.; Luthi, H. P. *J. Chem. Phys.* **2001**, *114*, 3949. ^b The present study. ^c *Advanced Inorganic Chemistry*; Cotton, F. A., Wilkinson, G., Eds.; John Wiley and Sons: New York, 1980.

isorbed on a (2 × 1)-reconstructed, hydrogenated (100) diamond surface.²³ A wide range of such molecular adsorbates were found to be able to accept an electron from the diamond valence band.

The purpose of the present investigation has been, using the DFT approach under periodic boundary conditions, to theoretically study the electron transfer from a H-terminated diamond (100)-2 × 1 surface to an atmospheric adlayer consisting of H₂O molecules attached to the surface (and predominantly hydrogen bonded to each other). The effect of an acidic environment (i.e., by introducing H₃O⁺ in the atmospheric adlayer) on (i) the electron transfer reactions and (ii) a potential hole formation in the diamond has then been compared with the neutral situation (only H₂O in the adlayer). A two-dimensional infinite slab has been used in modeling the H-terminated diamond (001)-2 × 1 surface, with the purpose of reproducing the frontal orbital interactions between a crystalline surface and molecular adsorbates.

Methods

The electronic and geometric structures of systems that are built up from the hydrogen-terminated 2 × 1-reconstructed diamond (001) surface and an aqueous adlayer have in the present study been calculated using first-principles density functional theory (DFT) and the program package CASTEP from Accelrys, Inc. One of the most commonly applied approximations in DFT, the local density approximation (LDA),^{24,25} assumes that the charge density varies slowly on an atomic scale. The most important deficiency of the LDA method is that it does not have the correct asymptotic behavior. Numerically, this overestimates the chemical bond energy in the system under investigation. A density gradient expansion is required to introduce inhomogeneity. Exchange and correlation effects have therefore in the present study been included within the generalized gradient approximation (GGA) developed by Perdew and Wang.²⁶ The atoms in the present investigation have been represented by ultrasoft nonlocal pseudopotentials in the Kleinman–Bylander fully separable form.²⁷ Moreover, the electronic wave functions were expanded in terms of plane waves and the electronic minimization was performed using a band-by-band conjugate-gradients minimization technique.²⁸ The specific *k*-points were generated by the Monkhorst–Pack scheme, which produces a uniform mesh of *k*-points in the reciprocal space.²⁹ Four *k*-points and a cutoff frequency of 300.0 eV have been used in the present investigation.

The performance of the exchange and correlation functional (PW91³⁰) used in this paper for the prediction of intermolecular interaction energies has been earlier evaluated on the basis of calculations on, e.g., hydrogen-bonded complexes like water.³¹ The calculated interaction energies show that the PW91 functional performs much better than other functionals like BLYP and B3LYP. The error in the binding energies was shown to be in the worst case less than 20%. In addition, the basis set dependence of the PW91 functional was observed to be relatively small. It was, therefore, shown that DFT using the PW91 functional is useful for the evaluation of dipolar interactions such as hydrogen bonds. Test calculations have also been

performed in the present study to further ensure the reliability of the present choice for a gradient-corrected electron correlation and exchange functional (GGA-PW91).

Since the evaluation of various DFT functionals in ref 31 was based on smaller complexes and the present study intends to model a heterogeneous solid/gaseous interface, it was found necessary to make a similar evaluation of DFT functionals for also solid systems. Consequently, test calculations have been performed on the hexagonal Ih phase of ice.³² As can be seen in Table 1, the GGA method that gives the most correct hydrogen-bond energy is the GGA-PW91 method: 17.6 vs ~21 kJ/mol for the experimental value. Furthermore, this method also results in calculated O···H–O bond lengths that are very close to the experimental ones (2.74 vs 2.76 Å). The other GGA functionals that were involved in this evaluation (RPBE³³ and PBE³⁴) showed larger discrepancies, especially when considering the bond energies: 12 vs 15 kJ/mol. Both the cell parameters and all the atoms in the cell were allowed to fully relax in the calculations using the BFGS algorithm (Broyden–Fletcher–Goldfarb–Shanno).³⁵ Since the usage of the GGA-PW91 method in the calculations resulted in good agreement with experimental observations (considering both bond energy and hydrogen-bond geometries), it was chosen as the most optimal gradient-corrected functional to use in the present investigation.

When a periodic boundary condition is used, two-dimensional infinite slabs are formed that are being separated by a vacuum level of various depths (Figure 1). A supercell is the smallest repetitive structural unit for all three spatial directions (*x*, *y*,

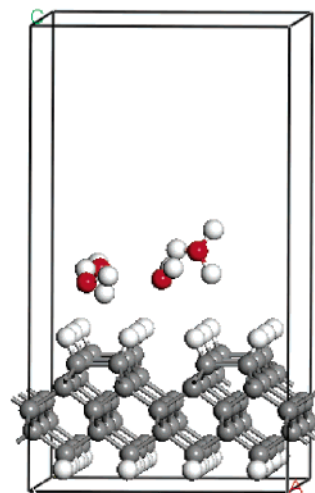


Figure 1. Supercell for modeling the hydrogen-terminated diamond (100)-2 × 1 surface with an attached acidic water adlayer (containing three H₂O molecules and one H₃O⁺ ion). The diamond slab consists of five carbon layers and one surface terminating hydrogen layer, each containing 12 atoms. The carbon dangling bonds at the backside of the supercell are passivated by an additional hydrogen layer of 24 atoms. This layer and the lowest nonreconstructed carbon layer are fixed during geometry optimization.

TABLE 2: Calculated Charges of the Separate Atomic Layers within the Supercell, Modeling the Upper Surface Slab of Diamond (100)-2 × 1^a

	charges in electrons		
	no adlayer	neutral adlayer	acidic adlayer
adlayer		0	−0.8
surface terminators	+3.4	+3.1	−0.5
first C layer	−3.5	−3.3	+0.5
second C layer	+0.1	+0.1	+0.1
third C layer	+0.1	+0.1	+0.5
fourth C layer	+0.1	+0.1	+0.4
fifth C layer	−5.7	−5.7	+0.7
underneath H layer	+5.5	+5.6	+0.1
electron transfer	0	0	1.8

^a With one exception, each layer consists of 12 atoms. There are 24 atoms in the underneath H layer. The charge of +0.1 for 12 atoms is within the limit of errors for the present theoretical method.

and z). Test calculations were here performed in which the (i) number of C layers, (ii) number of geometry optimized C layers, (iii) vacuum depth, and (iv) supercell edges *x* and *y* were varied. The effect of these parameters on the geometric structures and atomic charges (describing the degree of electron transfer) were then especially studied. The supercell shown in Figure 1 represents the converged cell for which only minor differences (<3% for the geometric structure and <2% for the atomic charges) were observed when two successive improvements of the parameters (i)–(iv) were used. Hence, the *x*-, *y*-, and *z*-edges of the supercell have been chosen large enough to avoid any appreciable interactions between neighboring water clusters (belonging to different cells). Even though a diamond surface coverage with water of at least one monolayer is expected under atmospheric conditions, the isolation of the water clusters in the model calculation by sufficient separation from each other is necessary since otherwise the periodic boundary conditions would lead to erroneous intermolecular bonding interactions in the resulting acidic, aqueous adlayer.

Results and Discussion

Hydrogen-Terminated Diamond (100). The electronic structure of the hydrogen-terminated 2 × 1-reconstructed diamond (100) surface (with no atmospheric adlayer being attached to it) has been calculated in the present study. The plane wave states have been projected onto a localized basis set to calculate atomic charges and bond population by means of Mulliken analysis.³⁶ The obtained charge distribution in the upper atomic layers of the diamond (100)-2 × 1 surface is demonstrated in Table 2.

The lower surface in Figure 1 is an unreconstructed one with the purpose of being able to distinguish between the two diamond surfaces in the partial density of states (PDOS) and density of states (DOS) curves. The larger number of lower H atoms is reflected in the larger dipole moment induced by the polar bonds of these H atoms to the fifth C layer. Moreover, the inherent limits of errors for the charge estimations in these calculations are about 0.01 electron per atom, which means that expected limit of error is about 0.12 electron for each atomic C layer in the model. Hence, within this error margin and aside from the discussed bond polarization effects, there is no induced charge and thus no indication for induced p-type conductivity within the slab C layers in the absence of an atmospheric adlayer. Early suggestions of surface states acting spontaneously as acceptors² are therefore not found for the hydrogenated diamond (100)2 × 1 surface in agreement with earlier band structure calculations.³⁷

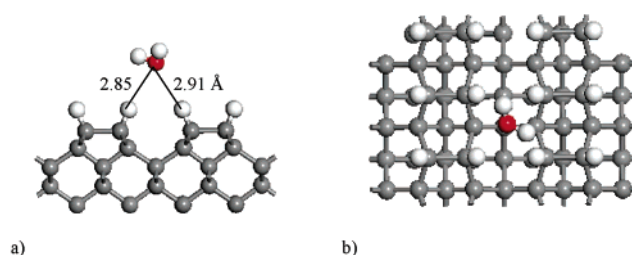


Figure 2. Resulting geometry (a, side view; b, top view) for the adsorption of H₂O to the H-terminated diamond (100)-2 × 1 surface. The supercell edges and the lower terminating H species are, for visualization purposes, not included in the figures.

Influence of an Aqueous Adlayer. General. Since it has experimentally been confirmed that an atmospheric situation will result in an induced p-type surface conductivity,^{6,16–21} a theoretical study has here been performed where the effect of an attached H₂O cluster on a potential electron transfer process (between the H-terminated diamond (100)-2 × 1 surface and the water adlayer) has been illuminated in more detail. The H₂O cluster (or adlayer) consisted of four water molecules. In the present study it was sequentially built up from one H₂O molecule to four H₂O molecules (with increments of one H₂O molecule), with the main purpose of investigating the relative strength of diamond–water and water–water bonds as a function of water cluster size. Water molecules are expected to become bonded to the hydrophobic H-terminated diamond surface with only very weak forces. To outline the influence of a more realistic temperature on the water geometry when attached to the present H-terminated diamond surface, a combined molecular dynamics (MD)/DFT^{38,39} simulation at room temperature was also performed using the CASTEP code from Accelrys, Inc. In this approach it is possible to simulate the motions of the atomic nuclei as they will occur, for example, in a chemical reaction while at the same time relaxing the electronic structure. A time step of 1 fs was used in the MD simulation, and the calculations were performed at the same level of accuracy as the other DFT-based calculations in the present investigation.

Surface–Water Interactions. The result of the geometry optimization for one physisorbed H₂O molecule on an H-terminated diamond (100)-2 × 1 surface can be seen in Figure 2. The oxygen atom in the water molecule became pointed downward (toward the diamond surface) with the closest O(H₂O)–H(surface) distance within the range 2.851–2.907 Å. The calculated adsorption energy for this finally obtained adsorbate structure was −15 kJ/mol (i.e., an exothermic reaction), which is within the energy range for physisorption. Water molecules are expected to become bonded to the hydrophobic H-terminated diamond surface with only weak van der Waals forces. Any barrier for the adsorption is not expected to be present due to the nature of this interaction. Moreover, the strength of the here calculated physisorption energy (−15 kJ/mol) seems not to be overcome by the thermal energy at room temperature (2.5 kJ/mol). However, since the solutions of the Schrödinger equations have here been based on a rigid structure at 0 K, an MD simulation at room temperature has also been performed to be able to confirm the predictions that a H₂O molecule will indeed become attached to the H-terminated diamond (100)-2 × 1 surface at room temperature. Within this simulation, the water molecule that was initially positioned about 4 Å above the H-terminated surface at room temperature (based upon $\Delta t = 0.2$ ps and a simulation including 200 iterations) became physisorbed to the surface with closest O(H₂O)–

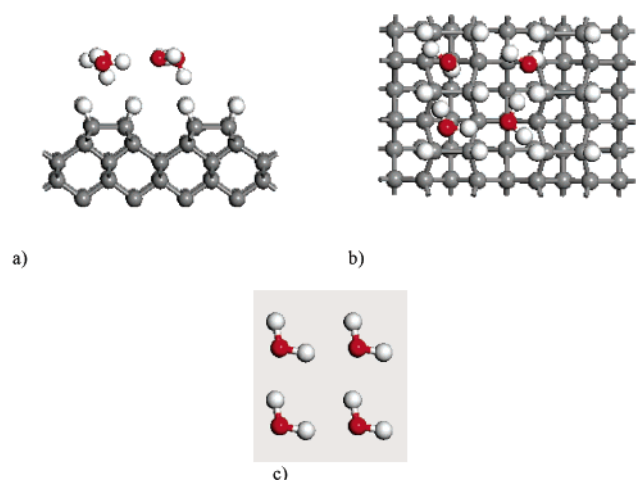


Figure 3. Resulting geometries (a, side view; b, top view) for the formation of four H₂O molecules attached to the H-terminated diamond (100)-2 × 1 surface. The hydrogen bond formation within the adlayer (b) is to be compared with the corresponding bond formation in the gaseous cluster containing four H₂O molecules (c).

H(surface) within the range 2.813–2.906 Å. Hence, there is hardly any noticeable deviation between the results obtained from 0 K DFT and room-temperature MD calculations regarding the structural geometry of physisorbed H₂O on H-terminated diamond (100)-2 × 1 surfaces.

The here presented energetic and structural results do not support any more pronounced hydrogen bond involvement in the water–diamond surface interaction. A hydrogen bond is an attractive, weak bond which is very special.³³ It forms when a hydrogen atom covalently binds to an electronegative atom (e.g., F, P, N) and is electrostatically attracted to another (typically electronegative) atom: X–H···X'. Very weak hydrogen bonds involving carbon can be formed in some systems. The strength of a hydrogen bond can be characterized by two geometric quantities that govern the hydrogen bond energy: collinearity of the X–H···X' atoms and optimal X···X' distance. The ideal, strongest hydrogen bond has its three atoms collinear. The strength of a hydrogen bond is usually less than 100 kJ/mol. However, the formation of a network of hydrogen bonds in, e.g., an atmospheric water adlayer on an H-terminated diamond surface, may lead to a cooperative effect that enhances the stability of the adsorbed layer considerably. The ease with which a diamond surface forms hydrogen bonds with a water adlayer determines the degree of hydrophilicity of that specific surface.

Surface–Water vs Water–Water Interactions. The cooperative effect of an atmospheric water adlayer was investigated by sequentially introducing a second, third, and fourth water molecule into the adlayer by translating a copy of the final geometry of the first adsorbed H₂O to a neighboring position on the H-terminated surface. The finally obtained geometries (after structural optimization) can be seen in Figure 3. An existence of many local minima on the potential energy surface for the water adlayer is expected due to the high degree of dynamics within this very weakly bonded adlayer. The above-mentioned procedure in the construction of the water adlayer was, hence, chosen to ascertain the modeling of the most stable water adlayer formation. As demonstrated in Figure 4, a decrease in averaged water–water hydrogen bond lengths was found to be strongly correlated with a decrease in averaged surface–water bond length when the number of H₂O molecules in the water adlayer was increased (bond lengths can qualitatively be used as measures of bond strengths). There was an obvious

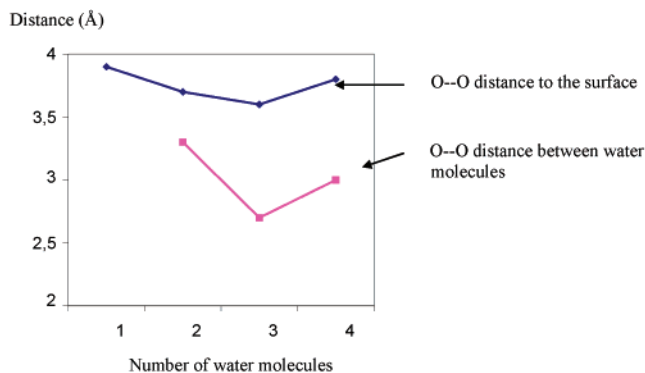
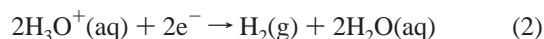
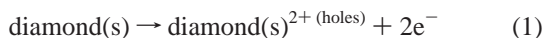


Figure 4. Surface–adlayer distance (C···O) versus intra-adlayer distances (O···O) as a function of H₂O molecules in the water adlayer. The C···O distances are calculated as the mean value over the distances between the individual water oxygen (four in total) and its closest surface C atom. The O···O distances are calculated as mean values between the neighboring H₂O pairs (four in total).

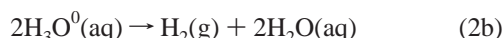
contraction of the water molecules in the adlayer, with a simultaneous transfer of the whole layer about 0.06 Å toward the surface (as compared to the distance of a single water molecule). The adlayer consisting of four H₂O molecules has a geometry that is somewhat different from the corresponding one for a gaseous water cluster containing four H₂O molecules. The geometry of the latter has also been calculated and geometry optimized in the present study. A four-membered planar ring was then formed with collinear O–H···O bonds of 2.8 Å. Hydrogen bonds are less dominant within the water adlayer on the diamond surface. Here, a nonplanar ring is formed with noncollinear O–H···O bonds of lengths between 2.7 and 3.6 Å. These structural differences indicate a weakening of hydrogen bonds within the water adlayer when the free water cluster approaches the diamond surface–water adlayer interactions.

Electron Transfer from a H-Terminated Diamond (100) Surface to a Water Adlayer. The total charge of the physisorbed water adlayer has been calculated for the adlayer consisting of four H₂O molecules by projecting the plane wave states onto localized basis sets. There was no observable electron transfer from the H-terminated diamond (100)-2 × 1 surface to the aqueous layer (see Table 2). This result is strongly supported by the experimental observations made by Vittone et al. which show that a weakly acidic water layer is demanded for p-type surface conductivity to occur.¹ As can also be seen in Table 2, the charge distribution within the H-terminated diamond surface is almost identical to the one obtained for the corresponding surface without any water layer attached to it. The physisorbed adlayer has only caused minor variations in the polarization of the C–H electric bonds on the surface. The lack of electron transfer between the H-terminated diamond surface and the water adlayer can be understood when studying the PDOS for the system. The LUMO level of the water adlayer (not attached to the surface) has an energy that is 3.7 eV higher than the HOMO level for the H-terminated diamond surface. This large difference in energy leads to an extremely small probability for an electron to be translated from the HOMO level of the surface to the LUMO level of the physisorbed water molecules. A similar result was also obtained by Goss et al. when they calculated the electronic properties of a variety of molecular physisorbed adsorbates using a DFT method and a cluster approach.²³ Their calculations resulted in an energy of –5 eV for the HOMO level of the H-terminated diamond (100) surface relative to the vacuum level, and a LUMO energy of –1 eV for a gaseous H₂O molecule.

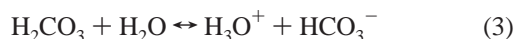
Effect of H_3O^+ in the Water Adlayer. *General.* The electrochemical surface transfer doping model proposed by Maier et al. involves, in addition to water molecules, also H_3O^+ as the most plausible electron-accepting ions in the attached adlayer on the H-terminated diamond surfaces.⁶ The doping mechanism is then assumed to involve the following red/ox reaction:



Equation 2 can be further divided into



The diamond valence band with and without two holes is expected here to play the role of the first red/ox couple involved in the red/ox reaction denoted by (1) and (2). The supply of hydronium ions is under common atmospheric conditions provided by the dissociation of carbonic acid:



The dominating ions in atmospheric aqueous layers are thus hydronium and the HCO_3^- anions. Note that for each hydronium ion that is neutralized by the doping reaction a corresponding anion remains in the wetting layer. It comprises the counter charge to the induced hole in the diamond and thus guarantees overall charge neutrality of the system.

Theoretical calculations have in the present study been performed to further elucidate these red/ox reactions to an atomic level of accuracy. One of the four H_2O molecules in the physisorbed adlayer was made acidic by adsorbing a proton to it ($\text{H}^+ + \text{H}_2\text{O} \rightarrow \text{H}_3\text{O}^+$). The construction of a supercell modeling this type of system can be made in different ways:

(i) A local counterion F^- (with fixed position and charge) is positioned at a large distance from the diamond slab (including its acidic water environment).

(ii) The diamond slab can be charged +1 by removing one electron from the HOMO level of the whole system. This upper energy level is located on the neutral H_3O adsorbate, and the removal of one electron will hence result in H_3O^+ . The program code itself provides a negative, compensating charge background to neutralize the supercells.

(iii) As a third alternative, the H_3O can exist in a cluster-based description of the diamond surface (without a supercell arrangement). The adlayer can then be made positively charged.

Almost identical results were obtained when all these possibilities were used in studying the degree of electron transfer for the situation with three H_2O molecules and one H_3O^+ ion in the adlayer. The occurrence of an electron transfer of about 1.5 electrons from the surface to the acidic, aqueous adlayer was observed. Either of the model construction types 1 and 2 has been chosen for the present investigation since the periodic boundary condition will preferentially be used in the present study (which excludes type 3).

Electron Transfer from a H-Terminated Diamond (100) Surface to an Acidic Water Adlayer. The total charge of the adlayer, consisting of three H_2O molecules and one H_3O^+ ion, has been calculated by projecting the plane wave states onto localized basis sets. An electron transfer of 1.52 electrons per unit cell toward the positively charged H_3O^+ ion was obtained,

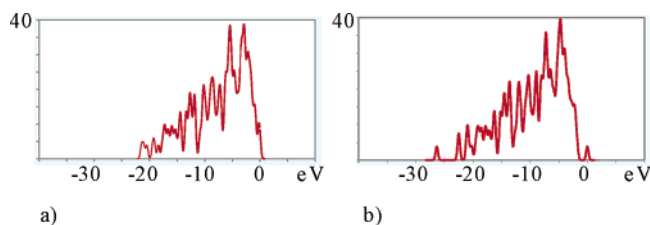


Figure 5. Density of states (DOS) for an H-terminated diamond (100)-2 \times 1 surface with a neutral water adlayer (a) and an acidic water adlayer (b).

causing severe bond-weakening effects in this adlayer species. The O–H bonds in the H_3O^+ ion have become elongated (from ~ 0.97 to ~ 1.03 Å), and the electron populations in the O–H bonds show negative signs (-0.30 – -0.52 $\text{e}/\text{\AA}^3$). These values have to be compared with the following for a “free” hydronium ion: 1.023 Å and 0.40 $\text{e}/\text{\AA}^3$, respectively. This indicates that local antibonding molecular orbitals in H_3O^+ have been partially filled, and then cause bond weakening (eventual disruption). A full modeling of the red/ox half-reaction 2 (i.e., including eq 2b) would require calculations of the accompanying activation barrier. Therefore, eq 2b was not included in the calculations. The bond weakening within the neutralized H_3O^0 may, however, be interpreted as the first step of a dissociation. Reaction 2b is thus hardly avoidable when two H_3O^0 molecules meet by surface diffusion.

Corresponding to the observed electron transfer, the induced holes in the diamond surface layer can also be characterized by the results of the calculations (under allowance for geometry relaxation). They are indicated as atomic charges in Table 2. There are now large differences between the atomic charges obtained in an H-terminated diamond (100) surface (with or without a neutral water adlayer) and those observed for this acidic water adlayer. The atomic layers beneath the upper C–H layer have obtained a more or less delocalized positive charge (hole formation).

It can also be observed in the DOS curve at the Fermi level of the acidic system (see Figure 5) that a peak about 22 eV above the lower edge of the valence band is present. The corresponding PDOS spectra may give information about those frontal orbitals that are capable of taking part in the interactions between the H-terminated surface and attached adlayer.⁴⁰ The PDOS spectra for the individual atoms in the adlayer, as well as PDOS spectra for some diamond surface atoms, can be seen in Figures 6–9. It is obvious from the individual PDOS curves that the peak at the Fermi level in the DOS curve is formed from an overlap of peaks both from the adlayer itself and from the upper H layer and the first C layer in the diamond surface. All of the individual molecules in the adlayer (with a strong emphasis on H_3O^+) are involved in this interaction. Not surprisingly, the surface-terminating H atoms directly attached to the attached adlayer are involved preferentially. The weight of the HOMO in PDOS spectra of the different atomic orbitals reflects the spread of the HOMO which acts as a surface acceptor for the diamond. As can be seen in Figure 9, a certain number of first layer C atoms will also contribute to this peak overlap. This circumstance speaks for an electronic (atomic) interaction including both the adlayer and the upper part of the diamond surface. This type of coinciding PDOS peaks is generally used as evidence for bond and molecular orbital (MO) formations.³¹ An observation that strongly supports the conclusion drawn from the PDOS curves is that the LUMO level of the free adlayer (which belongs to the low-energy antibonding MO in H_3O^+) is overlapping (in energy) with the HOMO level

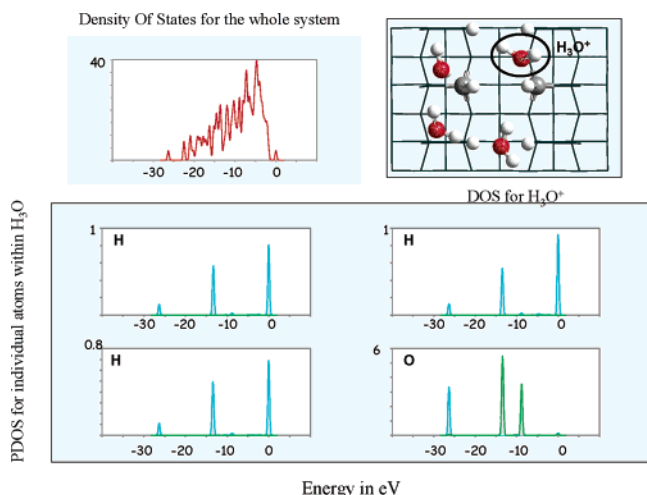


Figure 6. Contribution of the hydronium ion, in the acidic water adlayer, to the Fermi level peak in the total density of states for the whole system.

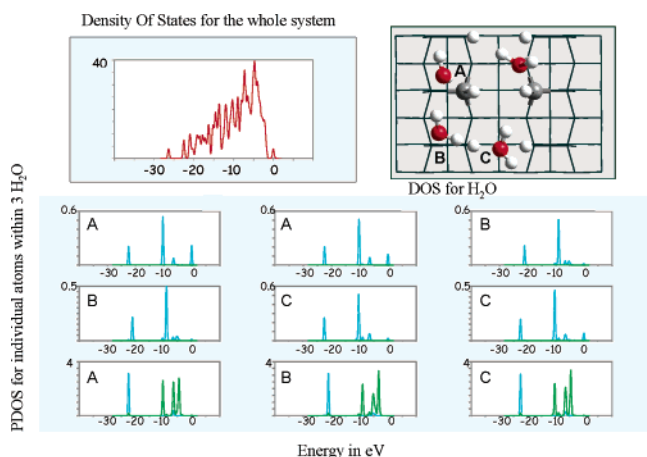


Figure 7. Contribution of the three water molecules in the adlayer to the Fermi level peak in the total density of states for the whole system. The lower three spectra show the oxygen peaks, while the others show the hydrogen peaks.

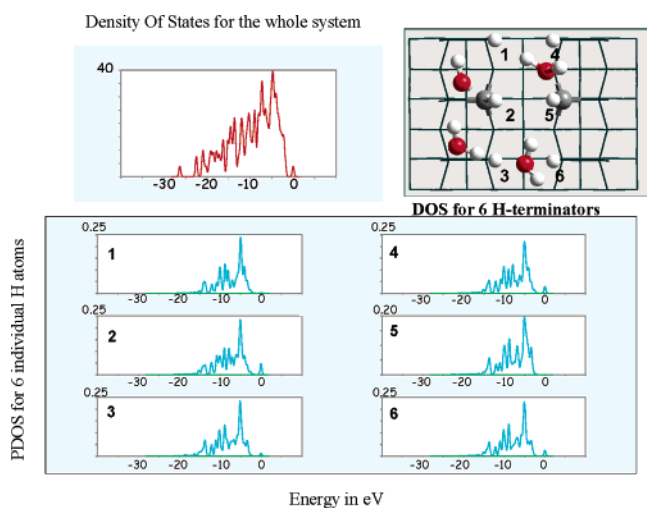


Figure 8. Contribution of the surface terminating hydrogens to the Fermi level peak in the total density of states for diamond with an attached water adlayer.

of the H-terminated diamond surface (Figure 10). The pronounced similarity in energetic positions will, hence, ensure a strong interaction between the two individual peaks: $\Delta E = |S_{ij}|^2 / (E_i - E_j)$, where S_{ij} is the calculated overlap integral for the

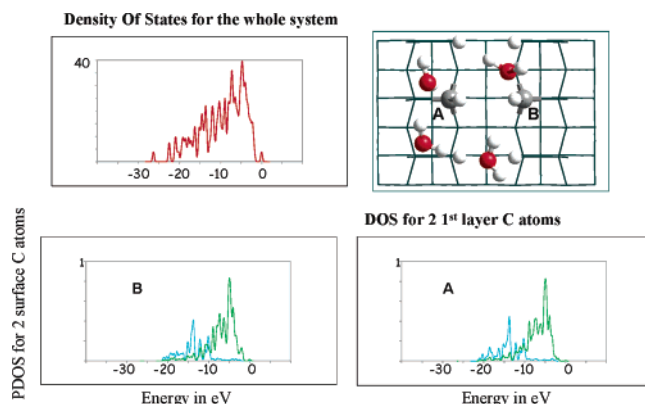


Figure 9. Contribution of some surface C atoms to the Fermi level peak in the total density of states for diamond with an attached water adlayer.

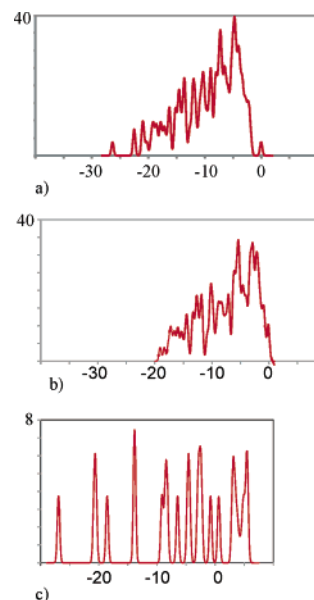


Figure 10. Density of states for the whole system (a), in addition to separate density of states for the H-terminated diamond surface (b) and acidic water adlayer (c). It can be shown here that the HOMO level for the diamond surface will overlap in energy with the HOMO level of the adlayer.

overlapping orbitals in the surface and adlayer, respectively.³¹ This result is to be compared with the corresponding situation with a neutral water adlayer, for which the LUMO level of the adlayer is situated above the HOMO of the H-terminated diamond surface.

Partial Density of States Analysis. Further insight into the mechanism of charge transfer between the diamond and the (neutral or acidic) aqueous adlayer can be obtained from the analysis of the density of states (DOS) and partial densities of states (PDOS) of the supercell system. Since the aqueous adlayer consists essentially of isolated molecules only weakly coupled to each other and to the diamond network, the PDOSs that belong to the atomic orbitals of the adlayer atoms will allow an interpretation in terms of molecular orbitals. This is demonstrated in Figures 6 and 7. Four subpanels show five of the system's PDOSs in Figure 6, i.e., those from projection onto the 1s orbitals of the three hydrogen atoms and onto the 2s (blue) and 2p (green) orbitals of the oxygen atom of the hydronium complex, respectively. Apparently, four PDOS peaks corresponding to the hydronium have substantial amplitude. The H_3O molecule essentially maintains the C_{3v} symmetry of the free ion. Consequently, the four PDOS peaks can be assigned to a

nondegenerate, mainly O 2s type molecular orbital (MO) at -27 eV, a 2-fold degenerate MO of mixed O 2p/H 1s character at -14 eV, a nondegenerate, mainly O 2p type orbital at -9 eV, and a nondegenerate mainly H 1s type orbital at 0 eV. The former three orbitals suffice to host the eight valence electrons of the H_3O^+ so that the MO at 0 eV is unoccupied for an isolated hydronium ion. In contact with the diamond surface it is, however, occupied and hosts the electrons transferred from the diamond. It constitutes the HOMO of the total system, and it also clearly shows up in the total DOS.

Further insight into the wave function of this HOMO is obtained from the PDOSs that correspond to the atomic orbitals of the water molecules of the adlayer (Figure 7). Again, blue spectra correspond to H 1s and O 2s, and green to O 2p character. The water molecules A, B, and C are almost, but not fully equivalent due to their different interactions with the diamond and with the hydronium. They maintain approximately the C_{2v} symmetry of the free molecule, and corresponding four nondegenerate MOs are easily recognized at -24 eV (mainly O 2s type), -10 and -6 eV (O 2s/H 1s type), and -4 eV (O 2p "lone pair" type). Interestingly enough, also a contribution of the system's HOMO is clearly identified in the H 1s PDOSs of the water molecules, the more pronounced the closer to the hydronium to the respective molecule is situated. This reflects the spread of the HOMO wave function over adjacent water molecules. This spread even involves the surface terminating hydrogen atoms in the vicinity of the hydronium complex, as demonstrated by the (H 1s type) PDOS of six H terminators in Figure 8. Due to the covalent bonding to the diamond slab those PDOSs already mimic the characteristic diamond DOS, but some show a very clear contribution of the system's HOMO at 0 eV.

Summarizing the PDOS analysis, it is thus stated that the HOMO of the combined diamond/adlayer system (after relaxation) is (i) situated in energy close to the valence band maximum of diamond, (ii) originates from the normally unoccupied LUMO of the H_3O^+ ion, (iii) is spread over adjacent water molecules of the adlayer, and (iv) is part of the surface terminating hydrogen atoms. This spread of the HOMO wave function is a direct albeit qualitative measure of the extent of transition of electrons from the diamond to the H_3O^+ . It also explains how the charge analysis in the preceding section could result in a noninteger number of electrons transferred per unit cell. The HOMO corresponds to two states per supercell volume (each occupied by one electron: spin-up or spin-down). However, only 90% of it is here found to be assigned to the adlayer, whereas the rest is counted to the diamond slab. This results in an only 1.8 electron transfer from the H-terminated diamond surface to the adlayer.

The sensitivity of a free diamond surface to ionic solutions and their pH values has earlier been demonstrated using ungated FET structures.^{41,42} The conductive surface channel was in direct contact with the liquid solution, forming a liquid gate. A p-type hydrogen-induced surface channel was one of the channels that were tested, and it was found to be gradually depleted with increasing pH (from 1 to 13). The mechanism of the pH sensitivity was believed to be related to interaction between the C-H surface dipoles and negatively charged species (e.g., OH^-) in the solution. However, due to the wide band gap, no charge transfer across the diamond-liquid interface was assumed to occur. The main difference between these earlier investigations and the present one is that we are not modeling a diamond/liquid interface here, but are modeling instead a diamond surface with an atmospheric acidic water adlayer attached to it. This

type of adlayer is too thin to represent a realistic liquid state. Hence, there are large possibilities for a totally different picture of the surface-adlayer interactions compared to a surface-liquid type of interaction. However, it would be of upmost importance to theoretically (using quantum mechanical calculations) study the effect of pH values on the surface conductivity for also diamond-liquid interfaces. The assumptions made in refs 41 and 42 could then be further grounded.

Summary and Conclusion

The exposure of hydrogen-terminated diamond surfaces to air has earlier been found to be a requirement for p-type surface conductivity to occur.^{6,20} The purpose with the present investigation has been to theoretically, using the DFT approach under periodic boundary conditions, study the electron transfer from an H-terminated diamond (100)- 2×1 surface to an atmospheric adlayer consisting of H_2O molecules physisorbed to the surface. The effect of an acidic environment (i.e., by introducing H_3O^+ in the atmospheric adlayer) on (i) the electron transfer reactions and (ii) induced p-type hole formations in the diamond surface layer have then been compared with the neutral situation (only H_2O in the adlayer).

The formation of a network of hydrogen bonds, e.g., in an atmospheric water adlayer on an H-terminated diamond surface, may lead to a cooperative effect that enhances stability considerably. The ease with which a diamond surface forms hydrogen bonds with a water adlayer determines the degree of hydrophilicity of that specific surface. An adlayer consisting of four H_2O molecules has been used in the present study. A geometry, somewhat different from the corresponding one for a gaseous water cluster, was obtained as a result of geometry relaxation. These structural differences indicate weaker hydrogen bonds within the water adlayer, which can be explained by the cooperative effect including also the diamond surface-water adlayer interactions. The calculated adsorption energy for this finally obtained adsorbate structure was -15 kJ/mol per water molecule (i.e., an exothermic reaction), which is within the energy range for physisorbed adsorption. Moreover, molecular dynamic simulations at room temperature gave hardly any noticeable change regarding the structural geometry for one physisorbed H_2O molecule on the H-terminated diamond surface.

A surface conductivity of p-type was found to be induced by an acidic environment. The total charge of an acidic water adlayer (consisting of three H_2O molecules and one H_3O^+ ion) was then calculated by projecting the plane wave states onto a localized basis set. An electron transfer of 1.8 electrons was observed to take place from the upper part of the surface valence band to the lower unoccupied level in the adlayer H_3O^+ , with a resulting delocalized hole formation in the upper surface C layers. A pronounced weakening effect of the H_3O^+ bonds was then also observed. These types of information were not found for an H-terminated diamond surface, with and without a neutral water adlayer attached to it.

The reduction part of the electrochemical reaction that takes place during the electron transfer process involves a decomposition of two hydronium ions to two water molecules and one hydrogen molecule. The hydronium ions are then expected to get in contact with each other via, e.g., "jumping" H ions. In addition, an activation barrier is expected to take place during this decomposition reaction, for which careful calculations of the transition state are required. This reaction process, together with the influence of these two neighboring hydronium ions on the electron transfer processes in total, is the scope for a future study.

Acknowledgment. The work was supported by the Swedish Research Council (VR) and Göran Gustafsson Foundation. The computational results were obtained using the software programs from Accelrys, Inc. (first-principles calculations were done with the CASTEP program within the Cerius² program package).

References and Notes

- (1) Landstrass, M. I.; Ravi, K. V. *Appl. Phys. Lett.* **1989**, *44*, 975.
- (2) Hayashi, K.; Yamanaka, S.; Watanabe, H.; Sekiguchi, T.; Okushi, H.; Kajimura, K. *J. Appl. Phys.* **1997**, *81*, 744.
- (3) Kawarada, H.; Aoki, M.; Sasaki, H.; Tsugawa, K. *Diamond Relat. Mater.* **1994**, *3*, 961.
- (4) Kawarada, H. *Surf. Sci. Rep.* **1996**, *26*, 207.
- (5) Hui, Jin-Lori; Pang, L. Y. S.; Molloy, A. B.; Jones, F.; Whitfield, M. D.; Foord, J. S.; Jackman, R. B. *Carbon (E-MRS '98 Meeting Symposium K: Carbon-Based Materials for Microelectronics)* **1999**, *37*, 801.
- (6) Maier, F.; Riedel, M.; Mantel, B.; Ristein, J.; Ley, L. *Phys. Rev. Lett.* **2000**, *85*, 3472.
- (7) Foord, J. S.; Chi Hian Lau; Hiramatsu, M.; Jackman, P. B.; Nebel, C. E.; Bergonzo, P. *Diamond Relat. Mater.* **2002**, *11*, 856.
- (8) Nebel, C. E.; Ertl, F.; Saurer, C.; Stutzmann, M.; Graeff, C. F. O.; Bergonzo, P.; Williams, O. A.; Jackman, R. B. *Diamond Relat. Mater.* **2002**, *11*, 351.
- (9) Kimura, K.; Nakajima, K.; Ymanaka, S.; Hasegawa, M.; Okushi, H. *Appl. Phys. Lett.* **2001**, *78*, 1679.
- (10) Bergmaier, A.; Dollinger, G.; Aleksov, A.; Gluche, P.; Kohn, E. *Surf. Sci.* **2001**, *481*, L433.
- (11) Goss, J. P.; Jones, R.; Heggie, M. I.; Ewels, C. P.; Briddon, P. R.; Öberg, S. *Phys. Rev. B* **2002**, *65*, 115207.
- (12) Takeuchi, D.; Riedel, M.; Ristein, J.; Ley, L. *Phys. Rev. B* **2003**, *68*, 41304(R).
- (13) Ristein, J.; Riedel, M.; Ley, L.; Takeuchi, D.; Okushi, H. *Phys. Status Solidi A* **2003**, *199*, 64.
- (14) Ri, S. G.; Tashiro, K.; Tanaka, S.; Fujisawa, F.; Kimura, H.; Kurosu, T.; Iida, M. *Jpn. J. Appl. Phys.* **1999**, *38*, 3492.
- (15) Vittone, E.; Ravizza, E.; Fizotti, F.; Paolini, C.; Manfredotti, C. Presented at the VIIIth International Workshop on Surface and Bulk Defects in CVD Diamond Films, Diepenbeek, February 2003.
- (16) Cannaearts, M.; Nesladek, M.; Haenen, K.; Stals, L. M.; De Schepper, L.; Van Heasendonck, C. *Phys. Status Solidi A* **2001**, *186*, 235.
- (17) Szameitat, M.; Jiang, X.; Beyer, W. *Appl. Phys. Lett.* **2000**, *77*, 1554.
- (18) Koslowski, K.; Strobel, S.; Ziemann, P. *Appl. Phys. A* **2000**, *77*, 211.
- (19) Riedel, M.; Ristein, J.; Ley, L. *Diamond Relat. Mater.* **2004**, *13*, 746.
- (20) Mantel, B. F.; Stammer, M.; Ristein, J.; Ley, L. *Diamond Relat. Mater.* **2001**, *10*, 1554.
- (21) Ristein, J.; Riedel, M.; Maier, F.; Mantel, B. F.; Stammer, M.; Ley, L. *J. Phys.: Condens. Matter* **2001**, *13*, 8979.
- (22) Ying Dai; Baibiao Huang; Dadi Dai. *Diamond Relat. Mater.* **2003**, *12*, 15.
- (23) Goss, J. P.; Hourahine, B.; Jones, B.; Heggie, M. I.; Briddon, P. R. *J. Phys.: Condens. Matter* **2001**, *13*, 8973.
- (24) Hammer, B.; Jacobsen, K. W.; Nørskov, J. K. *Phys. Rev. Lett.* **1993**, *70*, 3971.
- (25) Hu, P.; King, D. A.; Crampin, S.; Lee, M.-H.; Payne, M. C. *Chem. Phys. Lett.* **1994**, *230*, 501.
- (26) Perdew, J. P.; Wang, Y. *Phys. Rev. B* **1992**, *42*, 13244.
- (27) Kleinman, L.; Bylander, D. M. *Phys. Rev. Lett.* **1982**, *48*, 1425.
- (28) Teter, M. P.; Payne, M. C.; Allan, D. C. *Phys. Rev. B* **1989**, *40*, 12255.
- (29) Monkhorst, H. J.; Pack, J. D. *Phys. Rev. B* **1976**, *13*, 5188.
- (30) Perdew, J. P.; Wang, Y. *Phys. Rev. B* **1992**, *46*, 6671. White, J. A.; Bird, D. M. *Phys. Rev. B* **1994**, *50*, 4954.
- (31) Tsuzuki, S.; Luthi, H. P. *J. Chem. Phys.* **2001**, *114*, 3949.
- (32) Suja, H. *J. Chem. Phys.* **1985**, *82*, 424.
- (33) Hammer, B.; Hansen, L. B.; Nørskov, J. K. *Phys. Rev. B* **1999**, *59*, 7413.
- (34) Perdew, J. P.; Burke, K.; Ernzerhof, M. *Phys. Rev. Lett.* **1996**, *77*, 3865.
- (35) *Molecular Modeling and Simulation*; Antman, S. S., Marsden, J. E., Sirovich, L., Eds.; Springer-Verlag: New York, 2002; p 331.
- (36) Segall, M. D.; Shah, R.; Pickard, C. J.; Payne, M. C. *Phys. Rev. B* **1996**, *54*, 16317.
- (37) Kern, G.; Hafner, J.; Kresse, G. *Surf. Sci.* **1996**, *352–354*, 745.
- (38) Hohenberg, P.; Kohn, W. *Phys. Rev. B* **1964**, *864*, 136.
- (39) Payne, M. C.; Teter, M. P.; Allan, D. C.; Arias, T. A.; Joannopoulos, J. D. *Rev. Mod. Phys.* **1992**, *64*, 1045.
- (40) *Solids and Surfaces: A Chemist's View of Bonding in Extended Structures*; Hoffmann, R., Ed.; VCH Publishers: New York, 1988.
- (41) Denisenko, A.; Aleksov, A.; Kohn, E. *Diamond Relat. Mater.* **2001**, *10*, 667.
- (42) Mueller, R.; Denisenko, A.; Adamschik, M.; Kohn, E. *Diamond Relat. Mater.* **2002**, *11*, 651.